

Luminescence anisotropy of ZnO microrods

Volodymyr Khranovskyy, V Lazorenko, G Lashkarev and Rositsa Yakimova

Linköping University Post Print

N.B.: When citing this work, cite the original article.

Original Publication:

Volodymyr Khranovskyy, V Lazorenko, G Lashkarev and Rositsa Yakimova, Luminescence anisotropy of ZnO microrods, 2012, Journal of Luminescence, (132), 10, 2643-2647.

<http://dx.doi.org/10.1016/j.jlumin.2012.04.048>

Copyright: Elsevier

<http://www.elsevier.com/>

Postprint available at: Linköping University Electronic Press

<http://urn.kb.se/resolve?urn=urn:nbn:se:liu:diva-81813>

Luminescence anisotropy of ZnO microrods

V. Khranovskyy*¹, V. Lazorenko², G. Lashkarev² and R. Yakimova¹

¹*Linköping University, Department of Physics, Chemistry and Biology, 583 81 Linköping, Sweden*

²*Institute for Problems of Material Science, Krzhyzhanovskyy str, 3, 03142, Kiev, Ukraine*

Abstract

The local features of light emission from ZnO microrods were studied: it is revealed that ZnO luminescence spectra are significantly influenced by the crystal morphology. It is shown that the near and edge ultraviolet emission occurs primarily from the top (0001) planes of ZnO microrods; while the defect related visible emission was found to occur dominantly from the side facets. The room temperature cathodoluminescence analysis revealed that visible emission consists of a few overlapping peaks, arising due to recombination on common points and surface defects (Zn_i , V_o , V_o^0/V_o^{**} , V_o^{**} and surface defects.). While at low temperature, only the luminescence due to neutral donor bound exciton (D^0X) emission is observed. The data obtained suggest that the light emission spectra of ZnO material of diverse morphology can not be directly compared, although some common spectral features are present.

Keywords: ZnO microrods, Photoluminescence, Cathodoluminescence, NBE emission, DLE emission.

* Corresponding author: Volodymyr Khranovskyy, PhD
Semiconductor Physics, IFM
Department of Physics, Chemistry, and Biology
Linköping University
Sweden SE 58183
Phone local: +46-13-282663
Phone mob.: +46(0)737533927
Fax: +46-13-137568
Email: volkh@ifm.liu.se

1. Introduction

Zinc oxide is a prospective semiconductor material, being able to contribute significantly to such areas as transparent electronics [1], solid state lighting [2,3], gas [4] and bio sensors [5], energy harvesting etc [see, for examples 6 - 11]. It is a direct wide gap semiconductor ($E_g = 3.36$ eV at RT) with a large exciton binding energy (~ 60 meV), which inspires its applications as light emitting devices (LEDs). Therefore the light emission phenomena in ZnO have been a hot topic during the last decade. Particularly, the origin and nature of the visible luminescence in ZnO (so called “green-yellow” emission) are still under discussion. It is a general opinion that the visible luminescence is due to recombination of deep level defects, i. e. so called deep level emission (DLE). DLE typically is a wide band located at 450 - 660 nm, depending on a number of factors: crystal perfection, surface morphology, deviation from stoichiometry of the material, doping and impurities availability etc. Hence, at present a number of hypotheses exist for explanation of the DLE, often contradicting each other. For example, the green band is usually associated with the presence of oxygen defects. This includes oxygen vacancies (V_O), which are deep donors [9], or oxygen antisites (O_{Zn}), which are deep acceptors [10]. At the same time, Cu has also been claimed to be a possible source of green luminescence [12]. Eventually, oxygen excess has been associated with this band [13-15]. These examples illustrate the diversity of interpretations given for the visible luminescence in ZnO.

We suggest that not only chemical composition, stoichiometry or strain/stresses affect the luminescence properties of ZnO, but the morphology contributes significantly to its spectral properties. Apparently, ZnO luminescence spectra are complicated and consist of particular contributions from different areas of the studied material. This explains the spectral discrepancy of the luminescence spectra for ZnO objects of different morphology: polycrystalline films, epitaxial layers, nanostructures etc. In fact, different areas of ZnO structures may contribute qualitatively and quantitatively to the PL spectra.

Particularly, the anisotropy of ZnO light emission is facilitated by approaching nanoscale. Earlier Djuricic et al. reported that the majority of green emission centers are located at the surface of nanostructures [16]. Zhou et al. revealed that the different terminating facets exhibit different ratio of UV-to-green emission in cathodoluminescence (CL) spectra of ZnO nanostructures [17]. Foley et al. observed cathodoluminescence inhomogeneity between ZnO

microrod tips and sidewalls, accompanied by a variation in a chemical environment of surface oxygen ions [18]. Recently, we reported that the photoluminescence spectrum of individual horizontally located ZnO nanorod is different from the spectrum of similar nanorod array located vertically on the substrate [19].

In this work, we investigated the light emission anisotropy of ZnO microrods via cathodoluminescence mapping and low temperature micro-photoluminescence. The results demonstrate that the luminescence spectrum consists of different contributions from near band edge and deep level emissions, originating from different areas of hexagonally shaped ZnO microrods. It is shown, that the UV emission occurs mainly from the top planes of microrods, while the DLE originates from side facets and is of a complex nature.

2. Experimental details

ZnO microrods were prepared via Au assisted carbothermal reduction of ZnO powder on standard (100) oriented Si wafers. Prior to growth, a layer of 60 nm thick Au film was deposited on the substrate by radio frequency (RF) magnetron sputtering, being annealed at 500 °C for 45 min in vacuum afterwards, in order to coagulate the Au layer into droplets. ZnO powder (Sigma Aldrich 99.999 %) was mixed in equal proportions with graphite powder (Sigma Aldrich, 99 %) and placed in an alumina boat, then loaded to the center of a quartz chamber. The annealed Au/Si substrate was placed in the same boat. The ZnO microrods were grown at 850 °C under 25 sccm of argon flow during average time 30 min. The mechanism of VLS growth of the ZnO structures consists of several stages and is described elsewhere, e.g. [20]. The obtained ZnO microrods are single crystals, well faceted and having a diameter up to several microns and length up to several tens of micrometers. Scanning electron microscopy (SEM) was used to characterize the samples microstructure in a Leo 1550 Gemini SEM at operating voltage ranging from 10 kV to 20 kV and standard aperture value 30 μm . Cathodoluminescence (CL) spectra were taken at room temperature in the Leo 1550 Gemini SEM equipped with a MonoCL system (Oxford Instruments) using a 10 keV electron beam and 30 μm aperture with 1800 lines mm^{-1} grating. Cathodoluminescence measurements have been performed in panchromatic and monochromatic modes at room temperature. The fine luminescence properties of the ZnO microrods were investigated by micro-photoluminescence, carried out at 4 K by doubled frequency Nd:YVO 4

laser as continuous wave excitation source with the wavelength $\lambda = 266$ nm. The emitted light was collected and mirrored into a single grating 0.45 m monochromator equipped with a liquid nitrogen cooled Si-CCD camera with a spectral resolution of about 0.1 meV. The excitation density was ranged within $2 \div 400$ W/cm².

3. Results and discussion

Figure 1 presents a SEM image of ZnO microrods, possessing an average length around 30 μm and a width (rods outer diameter) around 3 μm ; thus, the length-to-width ratio was ~ 10 . The microrods are well faceted indicating single crystallinity and tend to be oriented with their c-axis perpendicularly toward the substrate surface. They were tightly located over the substrate surface with a density $\sim 2.25 \times 10^5/\text{cm}^2$.

In order to reveal the nature of the near band edge (NBE) emission we investigated the micro-photoluminescence (μPL) properties from the top of the sample at low temperature (4 K). Accordingly to the LT μPL spectrum (Fig. 2), the NBE luminescence is of excitonic type. The spectrum exhibits a number of well resolved peaks, which additionally proves the crystalline structure of ZnO microrods. The most intense peak at low temperature is due to neutral donor bound exciton (D^0X) emission, splitted into two, located at 3.3595 eV and 3.3563 eV. These peaks are labeled I_8 and I_9 lines respectively, and are believed to be due to the presence of Ga and In impurities [21]. This is because both Ga and In are similar to Zn in their atomic properties and are omnipresent impurities in ZnO. Toward the high energy direction, dominant peaks are accompanied by peak at 3.3665 eV, which is due to the ionized bound exciton emission (I_3 line) and weak evidence of the free excitonic emission can be observed at approximately 3.375 eV. Towards the low energy side, the spectrum possesses sharp line at 3.333 eV. This, according to the literature data is due to the exciton bound on structural defects (DBX), so called Y line [21]. Earlier, Dean [22] proposed a model for the origin of the Y-line to be caused by recombination at extended defects such as dislocation loops. Later it was observed in bulk and epitaxial ZnO samples that the DBX-line is mainly located in areas of crystal irregularities. It has been therefore concluded, that the DBX-line, similar to the Y and Z series observed by Dean in ZnSe [22] and the 3.41 eV recombination in GaN [23], is related to excitons bound at structural defects.

Two additional peaks of lower intensity, which however, may be recognized, are the

two-electron satellite (TES) recombination peaks of the neutral donor bound excitons (I_8 and I_9 lines). The low-energy part of the spectrum comprises the longitudinal phonon replicas (1LO, 2LO and 3LO, respectively) of the dominant peak I_8 , which are separated from it and between each other by 72 meV. Due to the faintly asymmetric shape and rather wide LO peaks we assume that they are results of overlapping of LO replicas of both dominant peaks – I_8 and I_9 . Photoluminescence analysis confirms that the microrods are of high structural quality, and the neutral donor bound exciton emission is dominant at low temperatures. This is specific for ZnO, since the free excitonic emission begins to be dominant above ~ 120 K [21]. However, presence of the Y line suggests availability of extended defects in ZnO structures. We have also performed the μ PL mapping over the length of the ZnO microrods, from roots to the tips (not shown here). It has to be noticed, that no significant difference in the PL spectra were observed during scanning of the ZnO rods length. The lowest luminescence intensity was observed in the regions near the substrate, which may be related to the increased concentration of non-radiative recombination centers at the ZnO/Si interface.

We acquired CL spectra from the ZnO microrods at room temperature (RT) in the wavelength range 300 – 750 nm (Fig. 3). As expected, the CL spectrum has a multi-peaked character: the narrow peak of ultraviolet (UV) emission was followed by so called “green-yellow” band of visible luminescence. The UV emission peak at $\lambda = 398$ nm is due to free excitonic emission (FX), possibly followed by longitudinal optical replicas of several orders (1st LO(FX), 2nd LO(FX) etc). The broad visible band consisted of several overlapped peaks, which we labeled as DLE 1 – 3. In order to determine the exact position of each peak, we applied the Gaussian fit.

As one can see from figure 3, the peak position of the NBE emission deviates from common ZnO energy band gap (3.36 eV) at room temperature. Such a low energy shift (“red” shift) may be due to increased contribution of the longitudinal phonon replicas, which can be observed at RT for high crystal quality ZnO. As it was earlier reported, the position of the near-band-edge emission at room temperature can vary significantly due to variations in relative contributions of free exciton emission and phonon replicas, which may be different for different growth conditions [10, 24]. Alternatively, the differences in position of the UV emissions could be due to significant concentrations of native defects in the ZnO [25].

Commonly, the ratio between the spectral integral intensity of NBE and DLE bands is

used ($I_{\lambda}(\text{NBE})/I_{\lambda}(\text{DLE})$) to estimate the contribution of recombination due to defect levels. Thus, for the ZnO microrods sample, studied in this paper, the $I_{\lambda}(\text{NBE})/I_{\lambda}(\text{DLE}) \approx 0.01$, i. e. DLE recombination significantly dominates over the NBE emission in the RT CL. Several different hypotheses have been proposed to explain the origin of the visible emission in ZnO, such as singly ionized oxygen vacancies [26-29], antisite oxygen [30], oxygen vacancies, zinc interstitials [31] and impurities [32, 33]. However, the origin of the visible emission is still rather controversial issue in ZnO. The peaks of visible emission at different positions may be assigned to different defects [34]. First, the observed shift of the NBE emission peak to lower energies could be due to contribution from the violet emission, which was reported to be at 3.08 eV and was assigned to oxygen antisite defect [35]. However, since the formation energy of proposed defect is too large, it makes it unlikely candidate to contribute to the emission band. The DLE 1 peak was observed at 479 nm (≈ 2.58 eV). The closest peak, reported earlier was at 2.5 eV attributed to the oxygen vacancy (V_o) [36]; while the peak at 2.7 eV was attributed to interstitial zinc defect (Zn_i) [36]. The specific feature of these defects is that they tend to exist simultaneously. Thus, taking into account the conditions of growth, it is reasonable to assume that the DLE 1 peak is due to a contribution of two defects: V_o and Zn_i .

Next DLE 2 peak is observed at 510 nm (≈ 2.43 eV). The common hypothesis for the origin of green emission is singly ionized oxygen vacancy [37]. However, accordingly to the theoretical calculations, oxygen vacancy is a deep donor, and singly ionized oxygen vacancies are unstable [38]. Later experimental results proposed that green emission at 2.45 eV is originated from a transition between neutral and double-ionized oxygen vacancy [39]. Another probable reason for it may be the surface defects or defect complexes [40].

Peak DLE 3 is located at 539 nm (≈ 2.3 eV): the closest peak, ever observed was at 540 nm and was explained by mechanism involving the oxygen vacancy [41]. Thus, green defect emission in ZnO nanoparticles has been attributed to a transition between electron near conduction band and a hole trapped at V_o^{**} level in the bulk of the particle, with the surface trapping of the photogenerated hole being the first step in the process [41]. Surface traps have not been conclusively identified, but oxygen has been proposed as a possible trapping site.

The peak DLE 3 has a tail, which is observed at the longer wavelength - around 580 ± 20 nm (≈ 2.14 eV). The possible reason for it may be oxygen atoms in interstitials (O_i) [42, 43] or

presence of hydroxyl groups on the surface [44]. However, hydroxyl groups may be present in the samples grown by low temperature approaches (as hydrothermal growth etc.) and are very unlikely to exist after the growth at 950 °C. We have summarized the peaks observed and their positions with the literature data in the Table 1.

Cathodoluminescence is a powerful technique for study the luminescent properties of micro/nanoscaled materials at high excitation range probing vertically the sample or mapping laterally the surface [45]. Study of the local structural features in comparison to the local light emission enables to reveal the effect of different type of structural defects (dislocations, grain boundaries etc.) on the *general* luminescence properties of the material. The mapping of the *total* spectral range light emission from the material is performed via panchromatic cathodoluminescence measurements. Moreover, the ability to acquire the luminescence signal at *certain* wavelength enables mapping of the material and visualizing the luminescence of defined wavelength, i. e. monochromatic cathodoluminescence mapping. It gives eventually the possibility to reveal the correlation of the luminescence nature and structural & morphological features of the material.

Earlier CL investigations of ZnO nanostructures have already shown that visible light is mainly emitted from the nanostructure surface region, while UV emission comes from the core [46]. This is in agreement with the calculations which indicate that dangling bonds at surfaces cause surface bands in the band structure of ZnO, which may affect its optical and electronic properties [47]. In order to investigate the local luminescence features, we acquired the CL monochromatic images, taken separately for certain wavelength, peculiar for NBE, DLE 1 – DLE 3 (Fig.4).

Due to the specific faceted morphology of every microrod, it was possible to probe the emitting characteristics of separate planes of hexagonal microrods. First, the clear correlation was observed between the microstructure and light emission: the areas which have structural defects, that are observed on the SEM image (Fig. 4a) are dark on the respective CL image of the NBE (Fig. 3b) as well as on any of DLE images (Fig. 4c,d,e,f). It evidences directly that these areas possess high concentration of non-radiative defects. Based on the brightness of the CL images (Fig. 4) one can clearly see that the contribution of the DLE 2 into the luminescence of ZnO microrods is the most significant (Fig. 4d) – it corresponds to the highest intensity peak in figure 3.

Moreover, a clear difference can be figured out from the NBE and DLE CL images (fig. 4b in comparison to Fig. 4c, d, e.): it is obvious, that the NBE emission occurs most intensively from the top planes (0001) of ZnO microrods; while the dominating DLE occurs from the side facets of the microrods. This implies that the edges of the microrods possess more deep level defects, responsible for the visible emission. Earlier, Djurišić et al. suggested that the green emission of ZnO nanostructures originated from surface defects [48]. Recently, Zhou has observed that the green emission is mostly emitted from the side planes of ZnO microcrystallites and therefore, it was concluded that the green emission mostly originated from the defects on/near the surface [49]. Therefore, our study agrees well with the previous reports. The DLE 3 emission was earlier reported, that it is not related on the surface, which is in agreement with our data (Fig. 4e) as well as with the previous results for ZnO samples sintered in moist air [50]. The NBE emission from the top (0001) planes of the ZnO hexagonal microrods may be additionally enhanced due to possible waveguide effects. Yang et al have observed the UV emission from both ends of the ZnO ribbon and almost no NBE emission signal was detected from the side surfaces, a clear indication of wave guiding of UV emission [51].

Conclusions

By using suitable spectroscopy and imaging techniques we have investigated the luminescence features of single crystal ZnO microrods, grown by VLS mechanism. It is shown that typically observed complex ZnO luminescence spectra are not only a result of different deep level defects recombination, but are significantly influenced by the crystal morphology. It is revealed that the NBE emission occurs mostly from the top planes (0001) of ZnO microrods; while the DLE mainly occurs from the side facets of the microrods. The observed visible emission from ZnO microrods at room temperature consists of a few overlapping peaks arising due to recombination on common points and surface defects. At low temperature only the luminescence due to neutral donor bound exciton (D^0X) emission was observed. The data obtained suggest that the light emission spectra of ZnO of diverse morphology can not be directly compared; although some common spectral features are present. Thus, the anisotropy of the ZnO luminescence is essential factor that should be taken into account for the design of relevant optoelectronic devices.

Acknowledgements

We greatly acknowledge the Linköping Linnaeus initiative for Novel Functional Materials (LiLi-NFM) for the support of this work.

References

- [1] V. Khranovskyy, U. Grossner, V. Lazorenko, G. Lashkarev, B.G. Svensson, R. Yakimova, *Superlat. Microstruct.* 42 (2007) 379-386.
- [2] V. Khranovskyy, G. R. Yazdi, G. Lashkarev, A. Ulyashin and R. Yakimova, *Phys. Stat. Sol. A* 205 (2008) 144-149.
- [3] V. Khranovskyy, I. Tsiaoussis, G. R. Yazdi, L. Hultman and R. Yakimova, *J. Cryst. Gr.* 312 (2010) 327 – 332.
- [4] V. Khranovskyy, J. Eriksson, A. Lloyd-Spetz, L. Hultman and Rositza Yakimova, *Thin Solid Films* 517 (2009) 2073-2078.
- [5] L. Selegard, V. Khranovskyy, F. Söderlind, C. Vahlberg, M. Ahren, P.-O. Käll, R. Yakimova and K. Uvdal, *ACS Appl. Mater. Interf.* 2 (2010) 2128-2135.
- [6] M. Willander, O. Nur, Q. X. Zhao, L. L. Yang, M. Lorenz, B. Q. Cao, J. Z. Perez, C. Czekalla, G. Zimmermann, M. Grundmann, A. Bakin, A. Behrends, M. Al-Suleiman, A. El-Shaer, A. Che Mofor, B. Postels, A. Waag, N. Boukos, A. Travlos, H. S. Kwack, J. Guinard and D. Le Si Dang, *Nanotechnology* 20 (2009) 332001.
- [7] Ü. Özgür, Ya. I. Alivov, C. Liu, A. Teke, M. A. Reshchikov, S. Doğan, V. Avrutin, S.-J. Cho, and H. Morkoç, *J. Appl. Phys.* 98 (2005) 041301.
- [8] V. Khranovskyy, U. Grossner, V. Lazorenko, G. Lashkarev, B. G. Svensson, R. Yakimova, *Phys. Stat. Sol. (c)* 3 (2006) 780–784.
- [9] C. Klingshirn, J. Fallert, H. Zhou, J. Sartor, C. Thiele, F. Maier-Flaig, D. Schneider, and H. Kalt, *Phys. Status Solidi B* 247 (2010) 1–24.
- [10] B. Djuricic, A. M. C. Ng, X. Y. Chen, *Progr. Quant. Electr.* 34 (2010) 191–259.
- [11] Z. L. Wang, *Mat. Sc. Eng: R: Reports* 64 (2009) 33-71.
- [12] N.Y. Garces, L. Wang, L. Bai, N.C. Giles, L.E. Halliburton, G. Cantwell, *Appl. Phys. Lett.* 81 (2002) 622.
- [13] K. Vanheusden C. H. Seager, W. L. Warren, D. R. Tallant, J. A. Voigt, *Appl. Phys. Lett.* 68 (1996) 403.
- [14] F. Leiter, H. Zhou, F. Henecker, A. Hofstaetter, D. M. Hoffman, B. K. Meyer, *Physica B* 908 (2001) 308.
- [15] D.C. Look, J. W. Hemsky, and J. R. Sizelove, *Phys. Rev. Lett.* 82 (1999) 2552.
- [16] A. B. Djuricic, W. C. H. Choy, V. A. L. Roy, Y. H. Leung, C. Y. Kwong, K. W. Cheah, T. K. G. Rao, W. K. Chan, H. F. Lui, C. Surya, *Adv. Funct. Matter.* 14 (2004) 856.
- [17] X. Zhou, Q. Kuang, Z. Y. Jiamg, Z. X. Xie, T. Xu, R. B. Huang and L. S. Zheng, *J. Phys. Chem. C* 111 (2007) 12091.
- [18] M. Foley, C. Ton-That and M. R. Phillips, *Appl. Phys. Lett.* 93 (2008) 243104.
- [19] V. Khranovskyy, R. Yakimova, F. Karlsson, P.-O. Holtz, Z. N. Urgessa, O. S. Oluwafemi, J. R. Botha, Comparative PL study of individual ZnO microrods, grown by APMOCVD and CBD techniques – submitted to *Physica B* (2011)
- [20] R. T. Rajendra Kumar, E. McGlynn, M. Biswas, R. Saunders, G. Trolliard, B. Soulestin, J.-R. Duclere, J. P. Mosnier, and M. O. Henry, *J. Appl. Phys.* 104 (2008) 084309.
- [21] B.K. Meyer, *Physica B* 201 (2003) 340–342.
- [22] Dean. P. J. Dean, *Phys. Stat. Sol. (a)* 81 (1984) 625.
- [23] Z. S. Fischer, G. Steude, D. M. Hofmann, F. Kurth, F. Anders, M. Topf, B. K. Meyer, F. Bertram, M. Schmidt, J. Christen, L. Eckey, J. Holst, A. Hoffmann, B. Mensching, and B. Rauschenbach,

- J. Cryst. Growth 189/190 (1998) 556.
- [24] T. Voss, C. Bekeny, L. Wischmeier, H. Gafsi, S. B ¨ orner, W. Schade, A.C. Mofor, A. Bakin, A. Waag, *Appl. Phys. Lett.* 89 (2006) 182107.
- [25] X. Zhou, Q. Kuang, Z.-Y. Jiang, Z.-X. Xie, T. Xu, R.-B. Huang, L. S. Zheng, *J. Phys. Chem. C* 111 32 (2007) 12091–12093.
- [26] Z. L. Wang, X. Y. Kong, Y. Ding, P. Gao, W. L. Hughes, R. Yang and Y. Zhang et al., *Adv. Funct. Mater.* 14 (2004) 943–956.
- [27] J. Zniga-Prez, V. Muoz-Sanjos, E. Palacios-Lidn and J. Colchero et al., *Phys. Rev. Lett.* 95 (2005) 226105.
- [28] S.J. Henley, M.N.R. Ashfold and D. Cherns, *Thin Solid Films* 422 (2002) 69–72.
- [29] N. Oleynik, M. Adam, A. Krtshil, J. Blsing, A. Dadgar, F. Bertram, D. Forster, A. Diez, A. Greiling, M. Seip, J. Christen and A. Krost et al., *J. Cryst. Growth* 248 (2003) 14–19.
- [30] J.H. Shen, S.W. Yeh, H.L. Huang and D. Gan, *Scr. Mater.* 61 (2009) 785–788.
- [31] J.H. Shen, S.W. Yeh, H.L. Huang and D. Gan, *Thin Solid Films* 519 (2010) 549–555.
- [32] G. Kenanakis, M. Androulidaki, E. Koudoumas, C. Savvakis and N. Katsarakis et al., *Superlatt. Microstr.* 42 (2007) 473–478.
- [33] Z. X. Fu, C. X. Guo, B. X. Lin and G. H. Liao et al., *Chin. Phys. Lett.* 15 (1998) 457.
- [34] M. D. McCluskey, S. J. Jokela, *J. Appl. Phys.* 106 (2009) 071101.
- [35] B. Lin, Z. Fu, Y. Jia, *Appl. Phys. Lett.* 79 (2001) 943–945.
- [36] M. K. Patra, K. Manzoor, M. Manoth, S. P. Vadera, N. Kumar, *J. Lumin.* 128 (2008) 267–272.
- [37] K. Vanheusden, C. H. Seager, W. L. Warren, D. R. Tallant, J. A. Voigt, *Appl. Phys. Lett.* 68 (1996) 403–405.
- [38] A. Janotti, C. G. Van de Walle, *Appl. Phys. Lett.* 87 (2005) 122102.
- [39] D. M. Hofmann, D. Pfisterer, J. Sann, B. K. Meyer, R. Tena-Zaera, V. Munoz-Sanjose, T. Frank, G. Pensl, *Appl. Phys. A* 88 (2007) 147–151.
- [40] Djurii, A. B.; Choy, W. C. H.; Roy, V. A. L.; Leung, Y. H.; Kwong, C. Y.; Cheah, K. W.; Rao, T. K. G.; Chan, W. K.; Lui, H. F.; Surya, C. *Adv. Funct. Mater.* 14 (2004) 856.
- [41] A. van Dijken, E. A. Meulenkaamp, D. Vanmaekelbergh, A. Meijerink, *J. Phys. Chem. B* 104 (2000) 1715–1723.
- [42] J. Qiu, X. Li, W. He, S.-J. Park, H.-K. Kim, Y.-H. Hwang, J.-H. Lee, Y.-D. Kim, *Nanotechnology* 20(2009) 155603.
- [43] D. Li, Y. H. Leung, A. B. Djurii, Z. T. Liu, M. H. Xie, S. L. Shi, S. J. Xu, W. K. Chan, *Appl. Phys. Lett.* 85 (2004) 1601–1603.
- [44] K. H. Tam, C. K. Cheung, Y. H. Leung, A. B. Djurii, C. C. Ling, C. D. Beling, S. Fung, W. M. Kwok, W. K. Chan, D. L. Phillips, L. Ding, W. K. Ge, *J. Phys. Chem. B* 110(2006) 20865–20871.
- [45] V. Khranovskyy, G. R. Yazdi, G. Lashkarev, A. Ulyashin and R. Yakimova, *Phys. Stat. Sol. A* 205 (2008) 144-149.
- [46] X. Liao, X. Zhang, *J. Phys. Chem. C* 111 (2007) 9081–9085.
- [47] K.-F. Lin, W.-F. Hsieh, *J. Phys. D: Appl. Phys.* 41(2008) 215307.
- [48] Djurii, A. B.; Choy, W. C. H.; Roy, V. A. L.; Leung, Y. H.; Kwong, C. Y.; Cheah, K. W.; Rao, T. K. G.; Chan, W. K.; Lui, H. F.; Surya, C. *Adv. Funct. Mater.* 14 (2004) 856.
- [49] X. Zhou, Q. Kuang, Z.-Y. Jiang, Z.-X. Xie, T. Xu, R.-B. Huang, and L.-S. Zheng, *J. Phys. Chem. C* 111 (2007) 12091-12093.

- [50] M. Liu, A. H. Kitai, and P. Mascher, *J. Lumin.* 54 (1992) 35.
- [51] H. Q. Yan, J. Johnson, M. Law, R. R. He, K. Knutsen, J. R. McKinney, J. Pham, R. Saykally, and P. D. Yang, *Adv. Mater.* 15 (2003) 1907–1911.

List of tables

Table 1. Room temperature cathodoluminescence properties of ZnO microrods. The data obtained via Gaussian fitting of the CL spectra: peaks' position (λ), energy peaks' position (E), integrated spectral intensity (I), as well as possible reasons for the origin of the observed peak, as referred to the literature.

Tables

Table 1.

Peaks	λ , nm	FWHM, nm	I_λ , a.u.	E, eV	Origin	Ref.
NBE	398	18	0.97	3.11	FE+ELO	[10, 24]
DLE 1	479	19	3.8	2.59	Zn _i , V _o	[36]
DLE 2	510	27	6.9	2.43	V _o ⁰ /V _o ^{**} Surf.Def.	[37,39] [40]
DLE 3	539	107	60	2.30	V _o ^{**}	[41]

Figure captions:

Fig.1: Top view SEM images of vertically aligned ZnO microrods on Si substrate, prepared by Au assisted carbothermal reduction.

Fig.2: Low temperature micro-photoluminescence spectrum of ZnO microrods (4 K). The respective peaks of free exciton (FX), neutral donor bound excitons lines (I_3 , I_8 , I_9) and their two electron satellite peaks (TES) as well as phonon replicas are respectively indicated. The vertical axis is in logarithmic scale.

Fig. 3: The room temperature cathodoluminescence spectrum of the ZnO microrods. The respective NBE and DLE peak's positions are indicated. The green and red lines are Gaussian fit data.

Fig. 4: The results of cathodoluminescence mapping of the ZnO microrods: a) schematic of a ZnO rod grown on Si substrate; the main orientation planes of a hexagonal crystal are depicted b) top-view SEM image of the studied microrods c) panchromatic CL image for the range 300 – 700 nm of the microrods d) respective monochromatic CL image, taken at 480 nm (DLE 1) e) respective monochromatic CL image, taken at 510 nm (DLE 2) and f) respective monochromatic CL image, taken at 540 nm (DLE 3). The images are as taken, no contrast or brightness changes were applied.

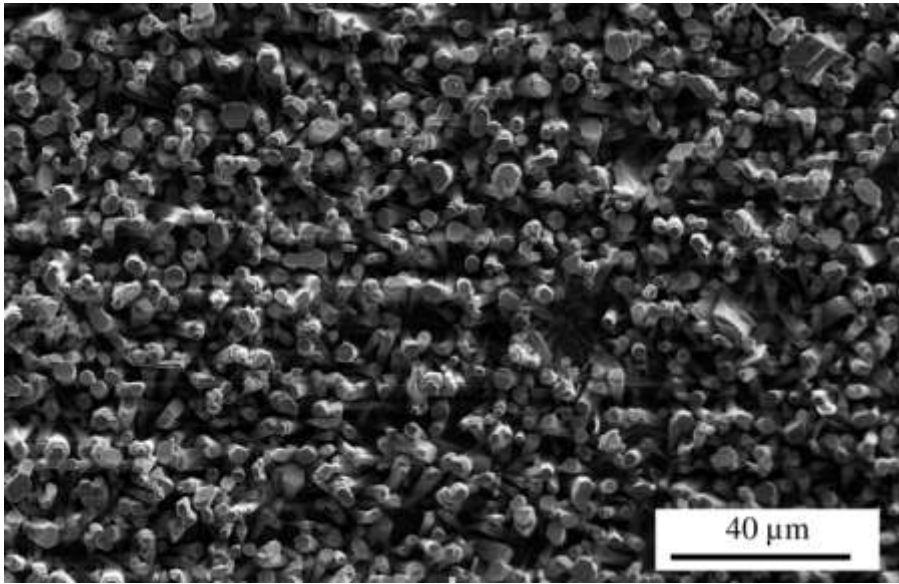


Fig.1: V. Khranovskyy *et al.*

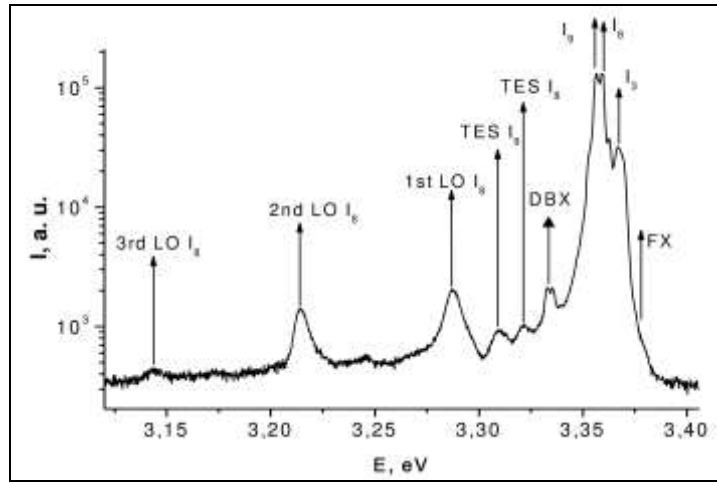


Fig.2: V. Khranovskyy *et al.*

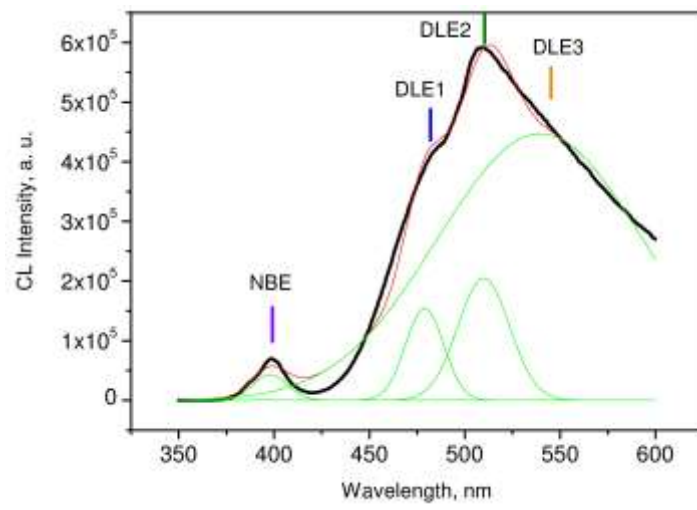


Fig. 3: V. Khranovskyy *et al.*

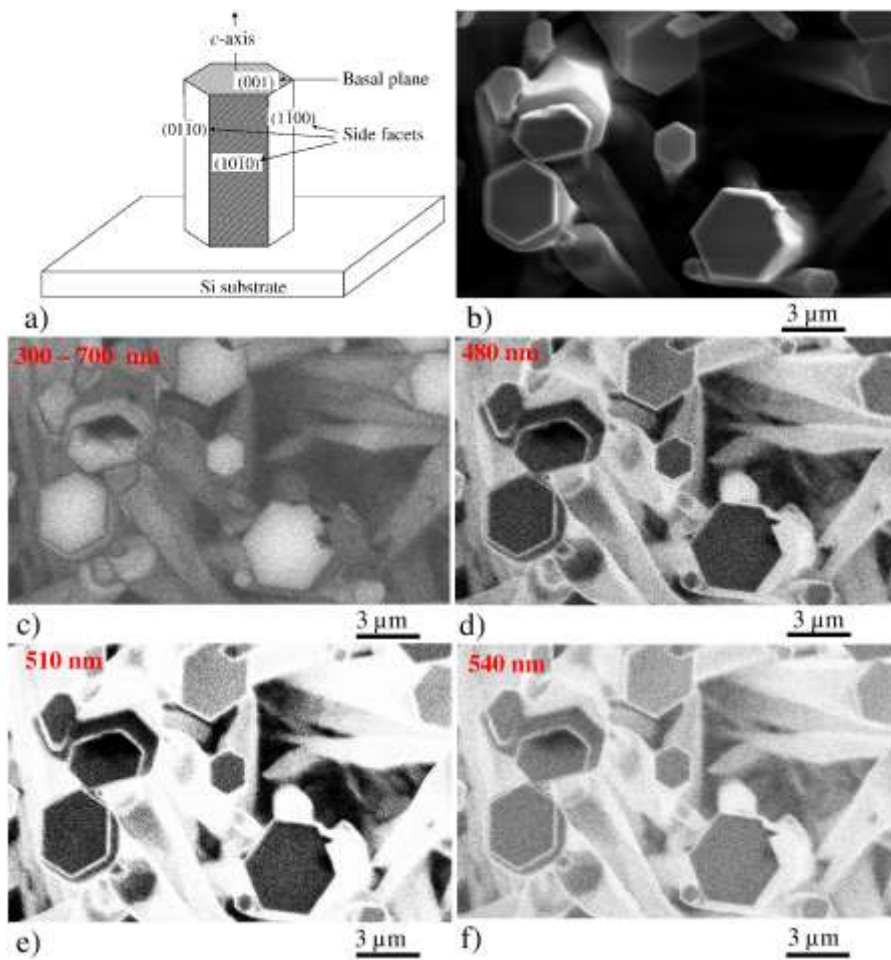


Fig. 4: V. Khranovskyy *et al.*